Advances in Concrete Construction, *Vol. 1, No. 3 (2013) 253-272*
DOI: http://dx.doi.org/10.12989/acc2013.1.3.253

Simulation of experiments on RC frames strengthened with dissipative steel links

Kyriaki Georgiadi-Stefanidi[1a], Euripidis Mistakidis[*] and Kosmas Athanasios Stylianidis[2b]

[1]*Laboratorty of Structural Analysis and Design, Department of Civil Engineering, University of Thessaly, Pedion Areos, GR-38334 Volos, Greece*
[2]*Laboratory of Reinforced Concrete and Masonry Structures, Department of Civil Engineering, Aristotle University of Thessaloniki, 54124 Thessaloniki, Greece*

(Received November 23, 2012, Revised February 25, 2013, Accepted April 18, 2013)

Abstract. The use of steel bracing systems is a popular method for the strengthening of existing reinforced concrete (RC) frames and may lead to a substantial increase of both strength and stiffness. However, in most retrofitting cases, the main target is the increase of the energy dissipation capacity. This paper studies numerically the efficiency of a specific strengthening methodology which utilizes a steel link element having a cross-section of various shapes, connected to the RC frame through bracing elements. The energy is dissipated through the yielding of the steel link element. The case studied is a typical one bay, single-storey RC frame, constructed according to older code provisions, which is strengthened through two different types of link elements. The presented numerical models are based on tests which are simulated in order to gain a better insight of the behaviour of the strengthened structures, but also in order to study the effects of different configurations for the link element. The behaviour of the strengthened frames is studied with respect to the one of the original bare frame. Moreover, the numerically obtained results are compared to the experimentally obtained ones, in order to verify the effectiveness of the applied simulation methodology.

Keywords: strengthening; non-linear analysis; concrete structures; earthquake engineering; finite elements method

1. Introduction

The strengthening of existing reinforced concrete (RC) buildings with pilotis (soft ground floor) is a current necessity in seismic prone areas. It is well known that the majority of these buildings were designed and built according to older codes. Moreover, they lack sufficient longitudinal and transverse reinforcement and their structural materials are either of low quality or exhibit degradation of their mechanical properties. As a result, these structures present weaknesses concerning their strength, ductility and stiffness. Strengthening this type of structures is essential in order to avoid damages or even loss of life from earthquakes.

*Corresponding author, Professor, E-mail: emistaki@uth.gr

http://www.techno-press.org/?journal=acc&subpage=7 ISSN:2287-5301(Print)2287-531X(Online)

One of the most popular methods for the strengthening of RC frames is the use of steel braces. A specific category of this strengthening type utilizes dissipative devices which exhibit a stable hysteretic behaviour and may sustain extensive plastification under the design earthquake. During the last decades significant research effort has been dedicated in this direction. For example, RC frames strengthened with a system of steel framed brace together with an elasto-plastic damper were tested by Kunisue *et al.* (1983). Failure was observed at the elasto-plastic energy dampers and the test results showed that the strength and the energy dissipation capacity can be significantly improved through this approach. Moreover, a calculation method was proposed for the estimation of the strength increase in strengthened RC frames and satisfactory approximation between experimental and analytical results was observed. Perera *et al.* (2004) performed tests in order to study the strengthening of masonry infilled RC frames. In some frames the masonry was replaced by a system of two steel braces and a vertical metallic link. Significant improvement of the energy dissipation capacity was observed. Pinto and Taucer (2006) conducted experiments on two full-scale, four-storey RC frames. High vulnerability to seismic loads was observed for the frame with no strengthening interventions. Moreover, it was found that strengthening with the use of steel braces significantly improved the seismic response and the energy dissipation capacity. A full scale, three-dimensional, two-storey RC frame strengthened with a bracing system was tested by Antonucci *et al.* (2006). Viscous dampers were employed and it was found that they can dissipate up to 95% of the induced seismic energy. The storey drift was also significantly reduced. Three tests were performed by D'Aniello (2006) on an existing RC building that was strengthened against seismic actions by the use of a system of two steel braces and a vertical dissipative link. From the test results it was concluded that shear elements can be easily connected to the concrete and the steel elements can also be easily replaced after a severe seismic event. A simplified simulation method was also applied and satisfactory approximation between analytical and experimental results was obtained.

Finally, the matter of upgrading of RC frames by means of innovative bracing systems seems to be a hot research topic and new methodologies evolve (Sickert *et al*. 2010). The use of a system of two steel braces with an ad-hoc designed dissipative element at the top, seems to be among the most preferred methodologies for RC frame upgrading.

In the present work the efficiency of a specific type of strengthening device, which consists of two steel braces connected to the RC frame through three different types of dissipative steel link elements, is investigated. The system studied here, may exhibit shear and/or flexural type of deformation and can increase the strength and the energy dissipation capacity of existing RC frames under seismic actions. An experimental program was carried out at the Laboratory of Reinforced Concrete and Masonry Structures of the Aristotle University of Thessaloniki, by Dr A.A. Karalis and T.N. Salonikios (Karalis *et al.* 2010, 2011, Karalis and Stylianidis 2013), under the supervision of the third author. From this program, eight specimens were selected as reference specimens in the present study. These specimens were tested under horizontal cyclic loading, four of them (one bare RC frame and three similar strengthened RC frames) without additional vertical loads at the columns and another identical group of four specimens with vertical loads.

In this paper, the study is focused on the numerical simulation of the tested specimens. All the tested RC frames are simulated numerically through effective two-dimensional finite element (F.E.) models, which are able to follow the highly non-linear nature of the problem (Abdollahi 1996, Rabczul *et al*. 2005, Wang *et al*. 2008). More specifically, appropriate two-dimensional finite elements are employed, which allow the detailed simulation of both the RC and steel link elements. Despite its phenomenological simplicity, the adopted simulation methodology allows the

consideration of the highly nonlinear phenomena that evolve and interact during the cyclic loading.

In the sequel, the numerical results are compared to the respective experimental ones. After the verification of the simulation models according to the experimental results, it will be possible to perform reliable "numerical tests" in order to investigate the effects of several parameters, reducing the required number of experiments. Of course, it has to be mentioned that the effectiveness of the adopted simulation methodology stems from the more or less two-dimensional deformation patterns that develop in the tested specimens. Similar methodologies have already been applied by the first two authors for the simulation of fibre reinforced cementitious matrix beams (Georgiadi-Stefanidi *et al*. 2010, 2011) and by the second author for the simulation of the response of various types of steel connections (Mistakidis *et al*. 1997, Kontoleon *et al*. 1999).

The paper is organized as follows; in the second Section the geometric and material properties of the various types of studied RC frames are presented. Moreover, the experimental setup, the instrumentation used and the loading procedure are described. The third Section deals with the principles of the applied numerical simulation. The fourth Section presents the numerical results for the different types of RC frames studied in this paper, in comparison with the respective experimental ones. Finally, the comparison between the overall behaviour of the examined types of RC frames is discussed in Section 5.

2. Types of RC frames studied and experimental procedure

2.1 Geometry and configurations of the studied specimens

The specimens studied in this paper represent a single-storey one-bay frame, rigidly based on a strong foundation and are constructed to a scale of 1:3. The RC part is exactly the same in all the tested specimens. The geometry of the specimens is shown in Fig. 1.

The frames are assumed to be constructed according to older regulations and thus, smooth steel rebars and widely-spaced stirrups were used, even within the critical regions of the possible plastic hinges. Moreover, the anchorage length of the steel bars of the beam does not meet the modern code requirements. The reinforcement arrangements for the beam and columns of the frame are depicted in Figs. 2 and 3, respectively.

The bracing system used for the strengthening of the RC frame is depicted in Fig. 4. It consists of two diagonal steel elements (bracings). Each bracing is connected to the corners formed by the lower ends of the columns and the base beam by external threaded rods. Moreover, the two braces are connected together at their other ends by means of a steel plate assemblage. On top of this, the lower end of the steel link element is connected. The upper end of the link element is connected to the midpoint of the RC beam through an appropriate arrangement of U-shaped steel plates which surround the beam and are connected to it by six passing-through bolts. It is pointed out that the latter steel plates, the two braces and the connections to the beams and the columns are purposely overdesigned and are not considered as parameters under investigation in the present study.

Four different specimen types were tested. Specimen type T1 is the bare frame, which is used as a reference for the evaluation of the strengthened frames. In order to allow the direct comparison, the bracing system was installed also in the bare frame (as in the strengthened specimens) but without the link element. It must be noted that due to the configuration of the

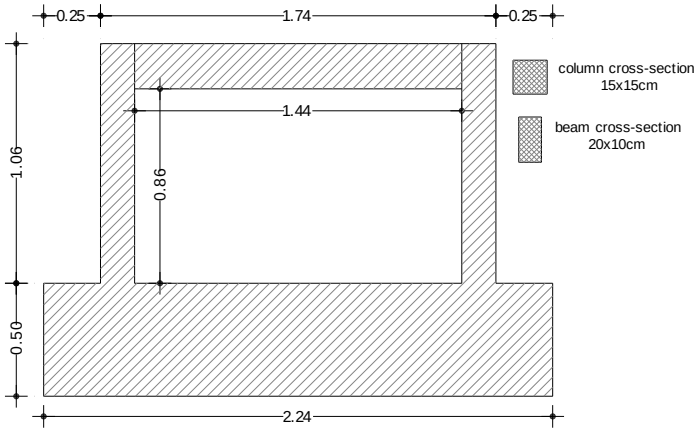

Fig. 1 Geometry of the specimens (dimensions in m)

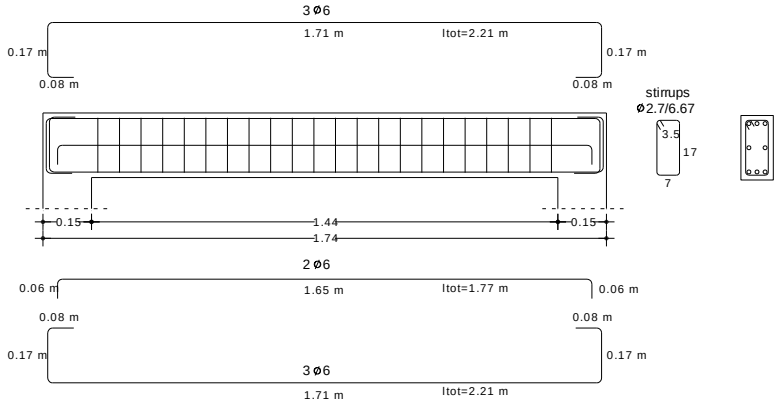

Fig. 2 Reinforcement arrangement for the beam

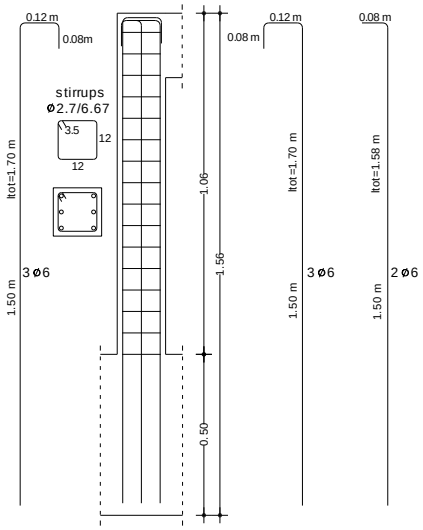

Fig. 3 Reinforcement arrangement for the columns

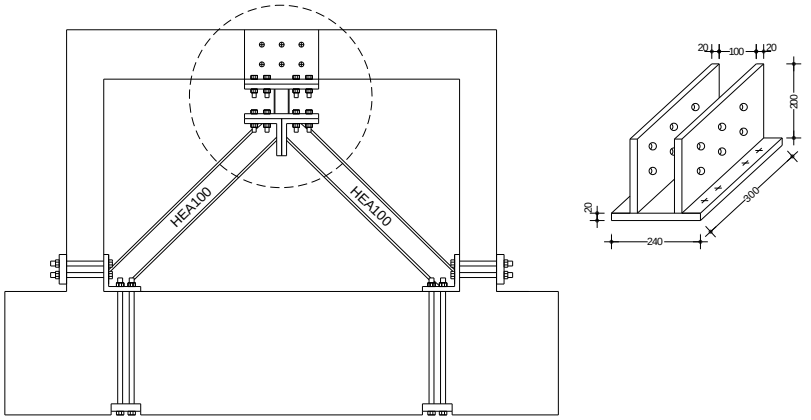

Fig. 4 Specimens strengthened by the steel bracing system and a steel link element at the top

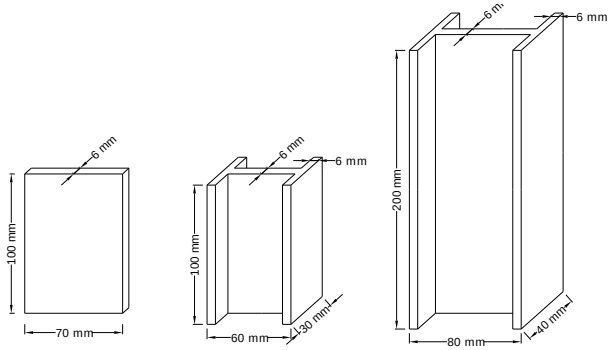

Fig. 5 The dissipative steel link elements of the strengthened frames T2, T3 and T4, respectively

bracing system and its connection to the columns, the plastic hinges that would be normally formed at the lower part of the columns, in this specific case are expected to appear at the upper part of the brace and column connection. Therefore, the presence of the bracing system in the bare frame without the link element, although it remains practically inactive, ensures the same geometrical conditions (actual free height of the columns) for all the specimen types. Consequently, the plastic hinges appear at the same locations for all the studied frames.

In the strengthened specimens (types T2, T3 and T4), the bracing system was connected to the middle of the top beam through a steel link element. The links used in each specimen type are presented in Fig. 5. The first link, used in the type T2 specimen, is actually a rectangular plate, having cross section height d = 70 mm, thickness t = 6 mm and length l = 100 mm. The second link, used in the type T3 specimen, is a steel element that has a symmetrical I cross-section with total section height d = 60 mm, flange width b = 30 mm, flange and web thickness t = 6 mm and length l = 100 mm. The third link, used in the type T4 specimen, has also a symmetrical I cross-section with total section height d = 80 mm, flange width b = 40 mm, flange and web thickness t = 6 mm and length l = 200 mm.

The above four types of specimens (T1, T2, T3 and T4) were tested with and without additional vertical loading at the columns. Therefore, the total number of different specimens and tests was eight. The four specimens in which the vertical loading was present at the columns during the

testing are referenced as T1-A, T2-A, T3-A and T4-A, while the other four specimens that were tested without axial loading are referenced as T1-NA, T2-NA, T3-NA and T4-NA, respectively.

It must be noted that the intention of the research team regarding the RC frame was to simulate construction practices and materials that were used during the decades of the ‘70s and ‘80s. For this reason, a rather low strength concrete was used with a compressive strength of 16 MPa and a tensile strength of 2.1 MPa. However, for the steel rebars, it was impossible to find in the market low yield stress steel (i.e., with yield stress of the order of 200-250 MPa). Therefore, it was decided to follow the construction practice of that era by using smooth steel rebars (that are available in the market) but with higher yield strength. In order to achieve the target strengths for the RC members, longitudinal bars with small diameter, equal to 6 mm (Ø 6), were chosen. Respectively, for the transverse reinforcement of the frame, stirrups with a diameter of 2.7 mm (Ø 2.7) were used.

More details for the used materials are given in Section 3.

2.2 Experimental test setup

For the tests, the facilities of the Laboratory of Reinforced Concrete and Masonry Structures of the Aristotle University of Thessaloniki were used. A double acting actuator was connected at the top beam of the specimen in order to apply reversing horizontal displacements. The actuator was connected at the top of the specimen by a system of two stiff steel plates coming into contact with the vertical outer sides of the beam - column joints, which were connected to each other by four long threaded rods (see Fig. 6). Another actuator was connected to the system, to apply vertical loads on the columns through a stiff steel beam, in a “load control” mode. In order to allow free rotation at the connection points, beyond the 3D rotational hinges of the actuator at the ends of its length, two more rotational hinges were installed between the steel plates and the two top beam - column joints of the specimen.

The specimens were instrumented by the use of seven LVDTs, measuring the shortening and the elongation of the outer fibres at the ends of the left column, the top horizontal displacement of the specimen and the net horizontal displacement at the top and bottom ends of the steel link element. The measurements of the LVDTs together with the measurements given by the load shell of the horizontal actuator were recorded through a digital controller.

Fig. 6 Experimental setup

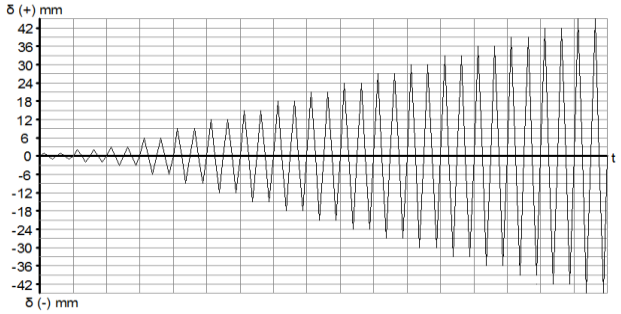

Fig. 7 Horizontal loading history

2.3 Loading procedure

The horizontal load was imposed in a "displacement control" mode. In total, 16 levels of displacement were used. Moreover, for each displacement level, two full cycles were imposed. The maximum value of induced displacement was 42 mm. The horizontal loading history is depicted in Fig. 7. Together with the horizontal displacement, a constant axial load of 80 kN was applied at the top of each column to the specimens T1-A, T2-A, T3-A and T4-A. The value of the axial load imposed on each column was actually equal to about the 20% of its load bearing capacity.

3. The principles of numerical simulation

The numerical simulation of the tested frames presented several difficulties due to the complexity of the problem and the existence of the following nonlinearities: (a) cracking and plastification of concrete, (b) yielding of the concrete rebars and (c) yielding of the steel link element. Moreover, while a three-dimensional model is expected to be more realistic and reliable due to the nature of its elements, it has the disadvantage of a high computational cost. Therefore, simpler two-dimensional models were formulated which, however, were able to capture in a rather accurate manner the overall behaviour of the studied problem (Rabczul*et al*. 2005, Wang *et al*. 2008).

3.1 Geometric and material properties

3.1.1 Concrete frame

The 2D simulation models of the RC frames consist of different types of finite elements, which are connected to the same grid of nodes:

- Plane stress F.E.: they were used for the discretization of the concrete volumes.
- Truss elements: they were used for the discretization of the longitudinal and transverse reinforcement.

Fig. 8(a) shows the discretization of the concrete frame, while Fig. 8(b) gives the layout of the longitudinal and transverse reinforcement.

The properties of the problem in the third direction (perpendicular to the modelling plane) were taken into account by assigning different thickness values to the respective finite elements. The

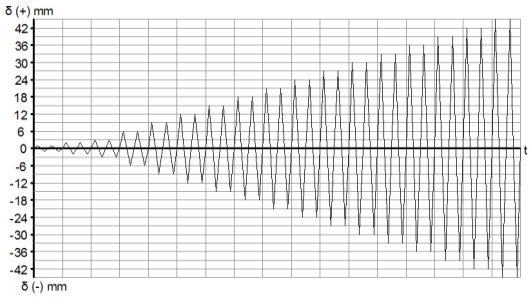

Fig. 7 Horizontal loading history

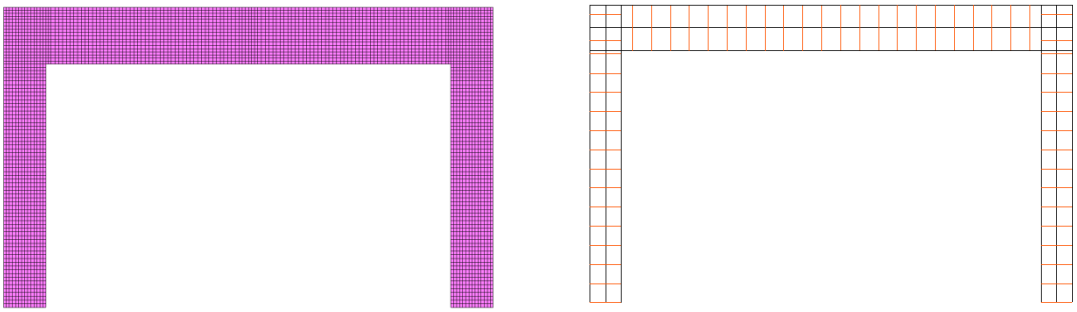

(a) F.E. mesh of the RC frame (plane stress elements)

(b) F.E. mesh of the longitudinal and transverse reinforcement (truss elements)

Fig. 8 The F.E. mesh of the simulation model

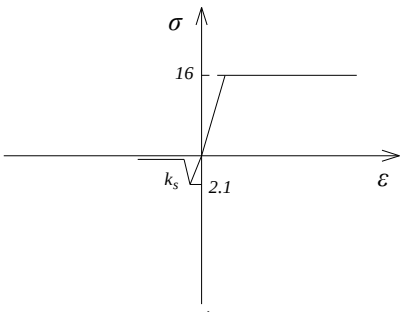

(a) Concrete

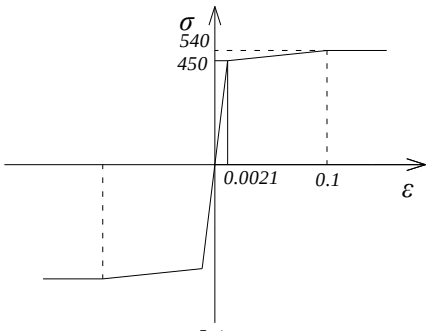

(b) Longitudinal steel reinforcement

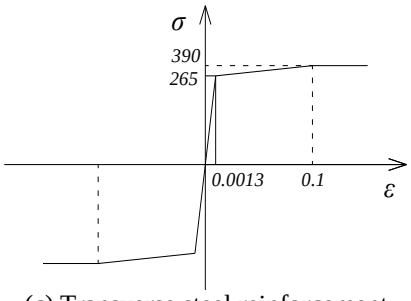

(c) Transverse steel reinforcement

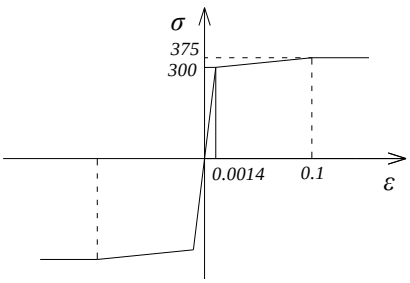

(d) Steel link elements

Fig. 9 Stress-strain relationships considered in the model

plane-stress elements representing the concrete beam and columns were assigned a thickness equal to the width of the corresponding cross-section, which is 100 mm and 150 mm for the beam and the columns, respectively. The cross-sectional area of the two-node, constant cross-section truss elements that represent the longitudinal and transverse reinforcement was taken equal to the total area of the corresponding reinforcing bars. That is, for the line of elements representing the top and the bottom steel reinforcement, the cross-sectional area was 3× 28.26 = 84.78 mm^2 (3Ø 6) and for those representing the middle longitudinal reinforcement, the cross-sectional area was 2 × 28.26 = 56.52 mm^2 (2Ø 6). For the elements representing the stirrups of the beam and columns, the cross-sectional area was 2 × 5.72 = 11.44 mm^2 in order to account for the two vertical legs of the Ø 2.7 stirrup.

The elements representing concrete were equipped with the stress-strain relationship of Fig. 9(a), which exhibits elastoplastic behaviour for compressive loading and a cracking behaviour for tensile loading. For the modelling of cracking in concrete, the smeared crack approach was followed (de Borst and Nauta 1985), i.e., the cracks were taken into account within each finite element in an average sense, by appropriately modifying the material properties at the integration points of the corresponding finite element. This approach involves no remeshing and is convenient when the crack orientation is not "a priori" known. The loss of tensile strength after cracking was modelled through a softening branch with a slope ks = 10^8 MPa. The elasticity modulus was taken equal to 28.4 GPa and the Poisson's ratio $v = 0.16$.

The longitudinal and transverse reinforcement bars were assumed to behave elastoplastically with hardening and were given a modulus of elasticity of 210 GPa and a Poisson's ratio $v = 0.20$. The stress-strain diagrams adopted for the longitudinal and transverse steel reinforcement are depicted in Figs. 9(b) and 9(c), respectively.

The one-dimensional laws of Fig. 9 are combined with an appropriate yielding criterion (von Mises for steel and Drucker-Prager for concrete), in order to take into account the other stress directions. Moreover, kinematic hardening was considered for the behaviour of steel after yielding, so that the Bauschinger effect is appropriately taken into account during load reversal.

3.1.2 Steel link elements

The link elements were simulated by the use of plane stress elements. A much denser finite element mesh (with respect to that used for the simulation of the concrete frame) was utilized. This was considered necessary in order to simulate as accurately as possible their behaviour, which dominates the strengthened systems. The two different F.E. meshes (the one corresponding to the RC frame and the one representing the link element) were connected through kinematical relationships, due to the fact that their nodes, at their common boundary, do not coincide.

The plane stress elements simulating the rectangular cross-section steel link element (T2 frame), were assigned a thickness of 6 mm, which is equal to the thickness of the link (see Fig. 10(a)). For the I-shaped cross-section steel links, the plane stress elements representing the flanges and those representing the web were assigned different thickness values. More specifically, for the second link (T3 frame) the elements representing its web were assigned a thickness of 6 mm and those representing the flanges were assigned a thickness of 30 mm (see Fig. 10(b)), whereas for the third link (T4 frame), the elements representing the web had thickness equal to 6 mm and those representing the flanges had thickness equal to 40 mm (see Fig. 10(c)).

The finite elements simulating the steel links were equipped with the stress-strain relationship given in Fig. 9(d), which exhibits elastoplastic behaviour with hardening. The elasticity modulus for these elements was taken equal to 210 GPa and the Poisson's ratio $v = 0.30$.

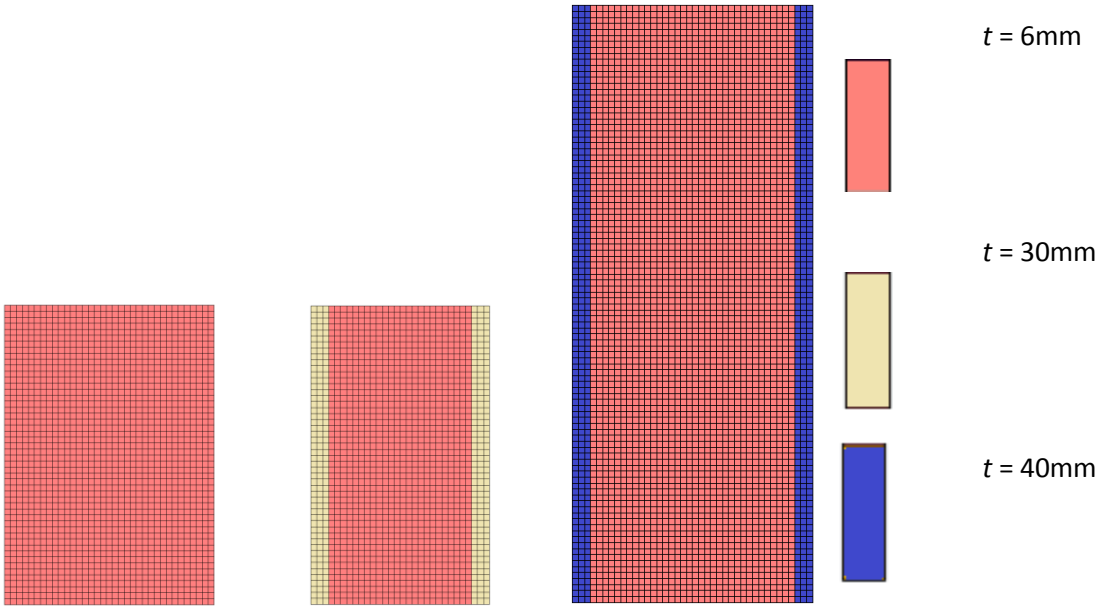

(a) T2 specimens (b) T3 specimens (c) T4 specimens

Fig. 10 Horizontal loading history

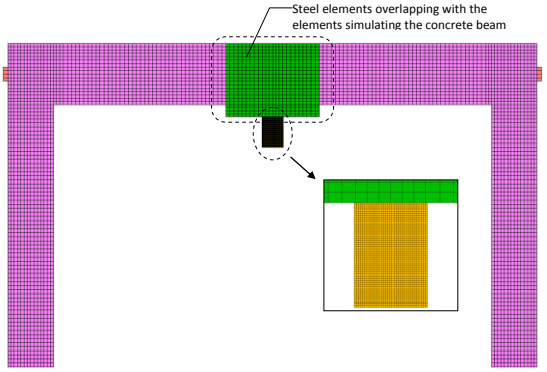

(a) Connection between the RC frame and the steel link

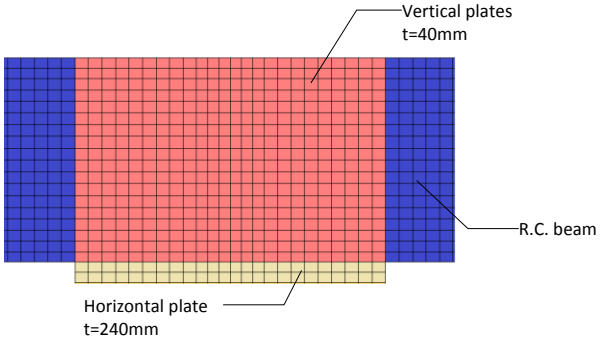

(b) Detail of the modeling of the collection plates

Fig. 11 The F.E. model

3.1.3 Connection between the RC frame and the steel dissipative link

As it was described earlier, the steel link element is fastened on the middle of the beam of the existing RC frame by means of an appropriate arrangement of steel plates and passing-through rods (see Fig. 4). This connection was simulated in the numerical model by attaching one more layer of finite elements, simulating the assemblage of the steel plates, on the layer of finite elements representing the RC frame. The two layers of elements are connected to common nodes, therefore there exists a continuous transfer of forces between them. At first, it seems that such a connection model is considerably different from the physical model where the steel plates are connected to the concrete with pass-through bolts. However, the fact that these bolts are prestressed, forces the connection to work, more or less, in a way similar to the one realized in the numerical model.

The resulting model is depicted in Fig. 11(a). A detail of the steel plates realizing the connection between the brace system and the existing frame is presented in Fig. 11(b). The elements representing the vertical side plates of Fig. 4 were assigned a thickness equal to 40mm, corresponding to the sum of the thicknesses of the two plates. The elements representing the horizontal plates of Fig. 4, the one belonging to the U-shaped arrangement and the other, which is connected to the first one and on which the link element is then welded, were assigned a thickness equal to 240 mm. All the aforementioned groups of elements were connected to common nodes so that they have common displacements.

The finite elements representing the plate assemblage were considered as elastic with elasticity modulus equal to 210 GPa and the Poisson's ratio $v = 0.30$. The reason for this simplification is the fact that these connection plates were purposely overdesigned and no damage was observed during the tests that took place.

3.2 Boundary conditions – loading procedure

All the specimens (T1, T2, T3 and T4) were subjected to horizontal cyclic loading, with and without additional vertical load at the columns. The cyclic load was applied incrementally in the form of induced displacement, whereas the constant vertical load was applied as a point load. The simulation of the load application procedure introduced several difficulties, which required a special numerical treatment. In general, it was not possible to apply the load directly to a nodal point of the F.E. mesh, due to the elastic-plastic and cracking properties of concrete. The following problems were noticed when following conventional load application procedures:

- When the applied load caused the formation of a compressive stress zone in the neighborhood of the load application node, stress concentrations and non-realistic stress fields occurred, creating excessive plastification of the elements representing concrete.
- During the load reversal, the applied load produced a tensile stress zone in the region of the applied load. Even for moderate load values, stress concentration appeared locally, near the node at which the load was applied. Therefore, non-realistic conditions for cracking were created, destroying the adjacent elements and leading to the premature termination of the numerical process.

To overcome the above numerical obstacles, a system of two steel plates was adopted: the first was introduced at the upper left and the second at the upper right side of the frame. Unilateral contact conditions were assumed between the plates and the frame. Moreover, the two plates were connected by kinematical constraints in order to achieve the load application in both directions and so that only compressive forces are imposed through the respective contact surfaces between the plates and the specimen. The above described loading procedures resulted in realistic stress and

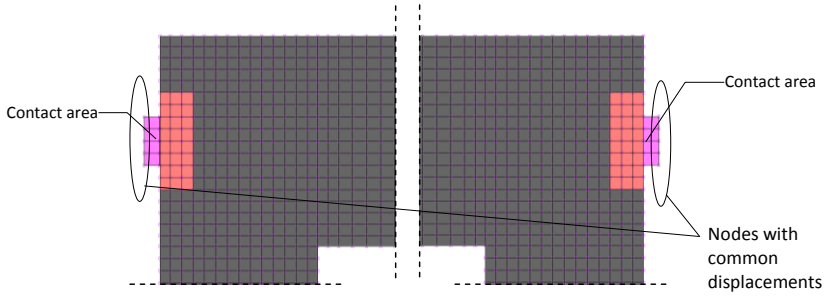

Fig. 12 The two-plate loading system

strain fields in the load application areas. Fig. 12 shows a detail of the two-plate system.

Finally, clamped supports were assumed at the positions where the steel rigid braces are connected to the frame and to the steel link.

3.3 Numerical solution procedure

The solution to the described numerical problem was obtained by using the software code MSC-MARC (2010). A Newton-Raphson iterative procedure was applied to handle the nonlinearities of the problem. The cyclic load was applied in the form of an induced displacement δ and the resulting force P at the points of the incrementally applied displacement was monitored. A relative convergence criterion equal to 0.01 was adopted, based on the residual forces.

4. Numerical results

Before displaying the numerically obtained results, it should be mentioned that for most of the cases treated here, it was not possible to simulate the performed experiments beyond a displacement of about 12 mm, due to numerical instabilities in the models, which led to the termination of the applied Newton – Raphson iterative procedure. The reason for the afore-mentioned behaviour was the significant damage of concrete that occurred for displacement values higher than 12 mm. For the same reason it was decided to simulate numerically only one load cycle for each displacement level instead of two similar cycles that were applied in the experiments. Therefore, the experimental P-δ curves used in this section for the comparison of the numerical with the experimental results are actually part of the complete response diagrams of each experiment. The numerical results will be presented and compared with the respective experimental ones in terms of load – displacement curves, skeleton curves that result from the aforementioned diagrams (consideration of first cycles only) and dissipated energy with respect to the imposed displacement for each studied specimen.

4.1 Results for specimen T1

The comparison between the numerical and experimental P-δ curves of the bare frame without axial force (T1-NA) and with axial force (T1-A) is presented in Fig. 13. Moreover, Fig. 14 presents the comparison of the P-δ skeleton curves obtained by the experiment and by the analysis

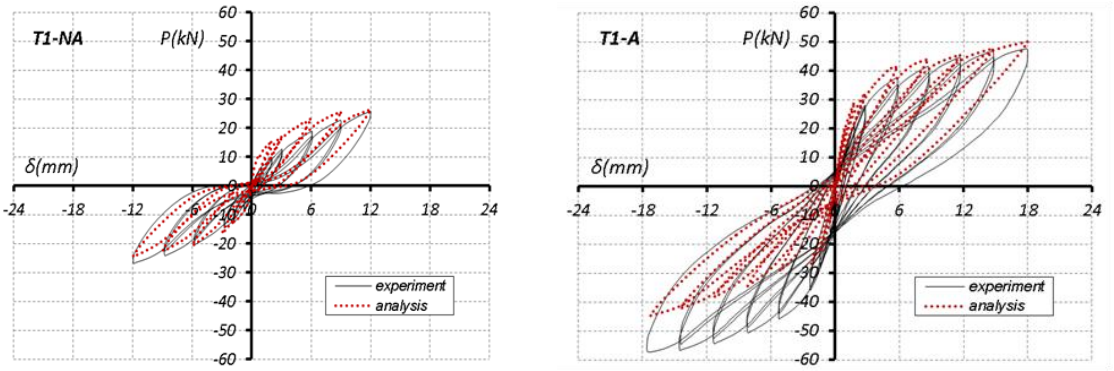

(a) T1 with no axial load (b) T1 with axial load

Fig. 13 Comparison of the numerical and experimental results for the T1 frames

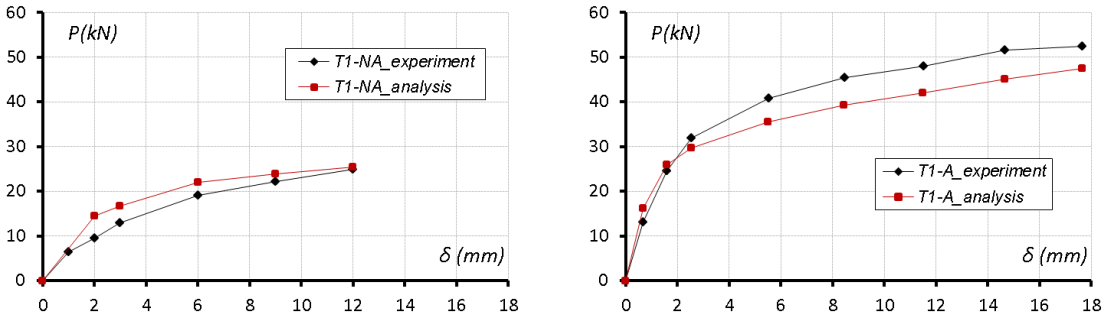

(a) T1 with no axial load (b) T1 with axial load

Fig. 14 Comparison of the P-δ skeleton curves obtained experimentally and analytically for the T1 frames

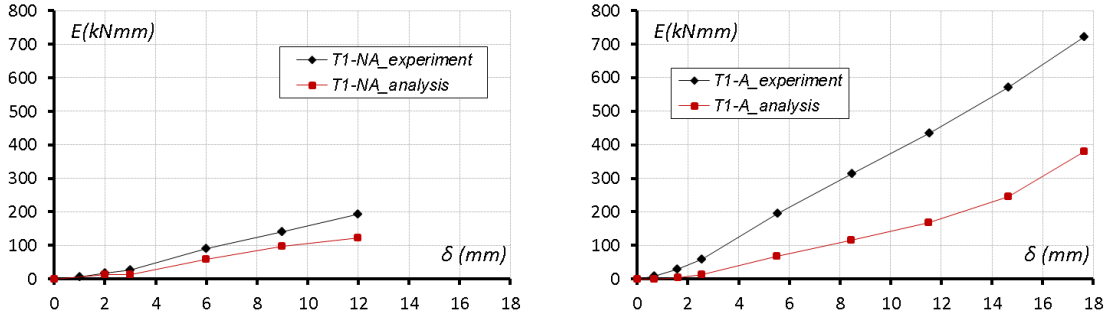

(a) T1 with no axial load (b) T1 with axial load

Fig. 15 Comparison of the numerical and experimental results for the dissipated energy of the T1 frames

of the T1-NA and T1-A frames. In the latter diagrams, only positive values are given for each applied displacement level, that correspond to the mean of the absolute values of the respective positive and negative cycles. It can be noticed that for the case of the T1-NA frame there is a good approximation between the numerical and the experimental P-δ curves. Consequently, there is a rather good agreement between the respective P-δ skeleton curves. However, the numerical model cannot approximate adequately the unloading branch of the experimental P-δ diagram, leading to

narrower hysteresis loops. The above can be attributed to the smeared crack approach that was used for the modelling of cracking, which cannot simulate accurately enough the closure of cracks and therefore, the behaviour of the specimen during the load reversal procedure. This deficiency of the numerical model is more obvious in the case of T1-A, where, except from the narrower hysteresis loops, one can notice differences between the load values *P* obtained for the negative cycles by the analysis and by the experiment. The aforementioned discrepancies are reflected also in the respective *P-δ* skeleton curves.

Fig. 15 gives the comparison of the dissipated energy in each load cycle. It can be observed that for the case of T1-NA the differences between the experimental and numerical values of dissipated energy are rather small and result from the narrower numerical hysteresis loops. However, for the case of the T1-A frame, the corresponding discrepancy is much wider, due to the additional differences in the negative load values.

4.2 Results for specimen T2

The overall behaviour of the T2 type strengthened frames is significantly improved due to the fact that the link element is immediately activated. Fig. 16 shows the P-δ curves for the T2-NA frame and for the respective T2-A strengthened frame, obtained by the numerical model together with the experimental results. Fig. 17 displays the corresponding skeleton curves. For the case of the T2-NA frame, it is noticed that there is a good agreement between the numerical and the experimental results, as far as the load values, the quality of the hysteresis loops and therefore, the overall behaviour of the specimen, are concerned. The small differences that arise in the obtained values can be considered acceptable, taking into account the highly nonlinear nature of the studied problem. In the case where axial load is imposed at the columns (T2-A frame), there is a good agreement between the numerical and the experimental results in terms of stiffness and quality of the hysterisis loops. However, some differences can be noticed between the numerical and the experimental results, mainly in terms of the obtained load values, especially during negative cycles. In Fig. 18 the numerical and experimental results for the dissipated energy for T2-NA and T2-A frames are presented. As expected, there is a very good agreement between the results for the T2-NA frame, whereas some differences arise for the T2-A strengthened frame, due to the above mentioned differences in the obtained values of the *P-δ* curves.

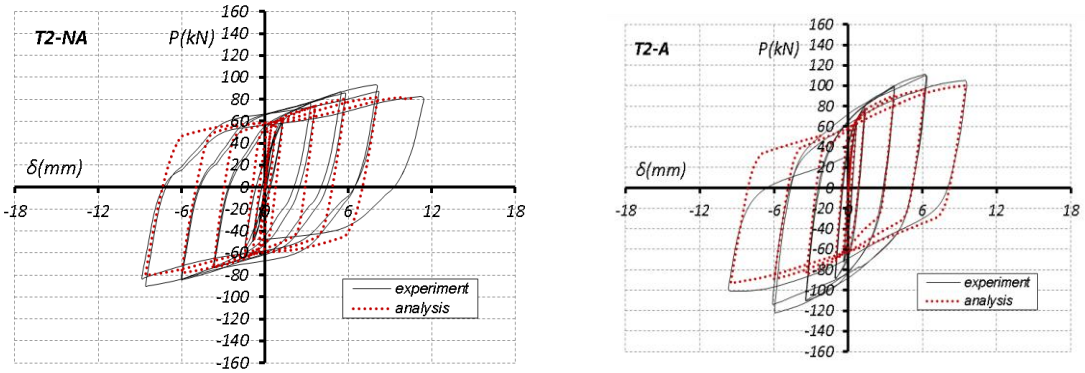

(a) T2 with no axial load (b) T2 with axial load

Fig. 16 Comparison of the numerical and experimental results for the T2 frames

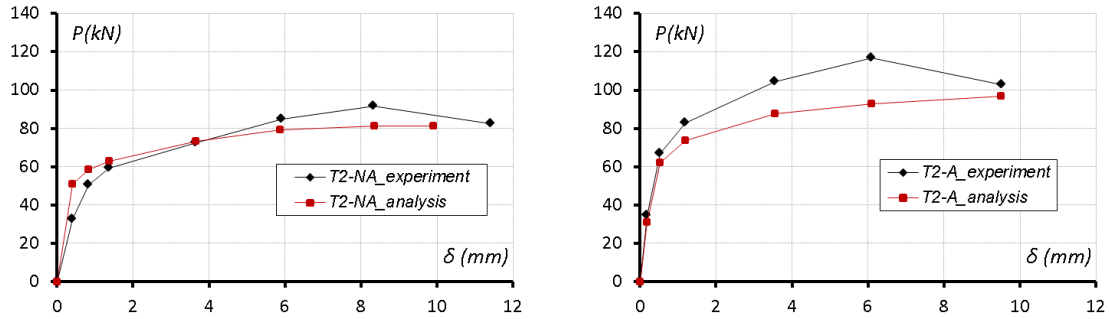

(a) T2 with no axial load (b) T2 with axial load

Fig. 17 Comparison of the P-δ skeleton curves obtained experimentally and analytically for the T2 frames

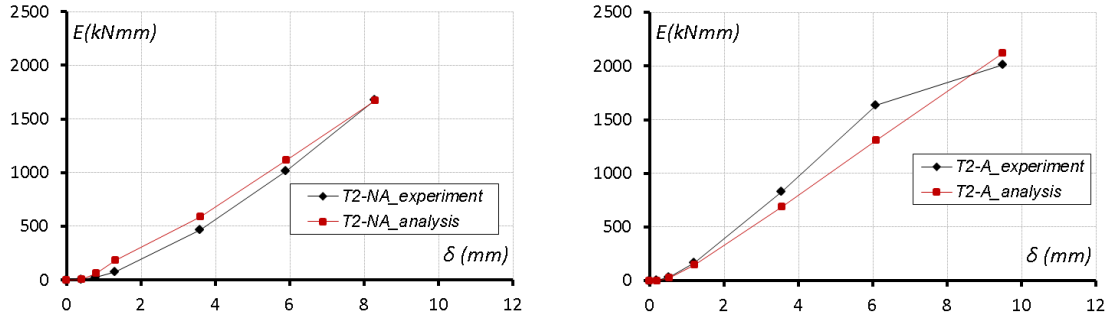

(a) T2 with no axial load (b) T2 with axial load

Fig. 18 Comparison of the numerical and experimental results for the dissipated energy of the T2 frames

4.3 Results for specimen T3

In this case, the RC frame was strengthened by the use of an I-shaped cross-section link element. Fig. 19 shows the experimentally and numerically obtained *P-δ* curves for the T3-NA frame (without axial load) and for the respective T3-A frame (with axial load). Moreover, Fig. 20 displays the corresponding skeleton curves. It is noticed that, for the case of the T3-NA frame, the *P-δ* curve obtained by the numerical analysis is similar to the corresponding experimental one, with respect to the stiffness of the system, the quality of the hysteresis loops and the behaviour of the specimen in general. A small difference is noticed concerning the load values P that correspond to the higher displacement values δ. More specifically, for this displacements range, the load values obtained by the numerical analysis are slightly lower than the respective experimental ones. This difference is also reflected to the comparative diagram of the *P-δ* skeleton curves depicted in Fig. 20.

In the case of the T3-A strengthened frame (with axial load imposed at the columns), there is a rather good agreement between the numerical and experimental results as far as the stiffness of the system and the quality (shape and width) of the hysterisis loops are concerned. However, some difference is noticed in the *P-δ* diagram (see Fig. 19), concerning the obtained load values for both the positive and negative load cycles. Due to this discrepancy, differences are also noticed between the numerical and the experimental P-δ skeleton curves. As it can be noticed in Fig. 20, the

numerical curve corresponds to lower load values P with respect to the experimental one, for the majority of the displacement values δ.

In Fig. 21, the values of the dissipated energy obtained by the analysis and the experiment are compared. For the case of the T3-NA strengthened frame it can be seen that the numerical and experimental results are almost identical. For the T3-A frame it can be concluded that for the lower displacement values δ there is a good agreement between the numerical and the experimental

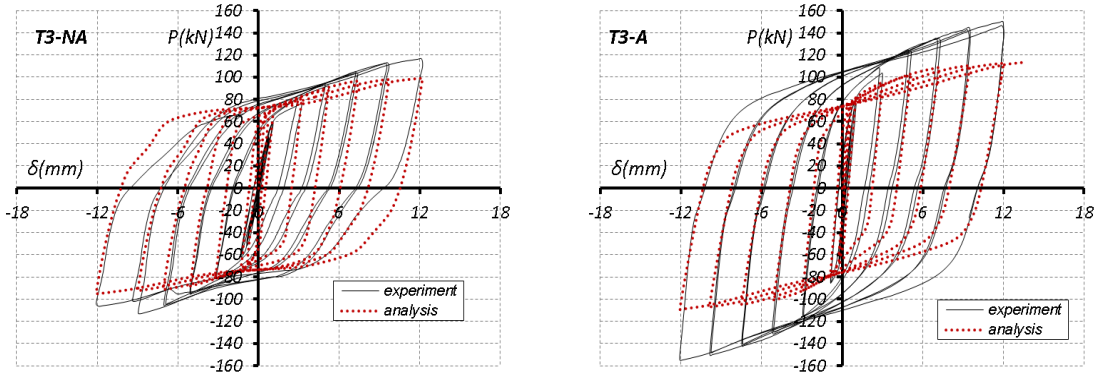

(a) T3 with no axial load (b) T3 with axial load

Fig. 19 Comparison of the numerical and experimental results for the T3 frames

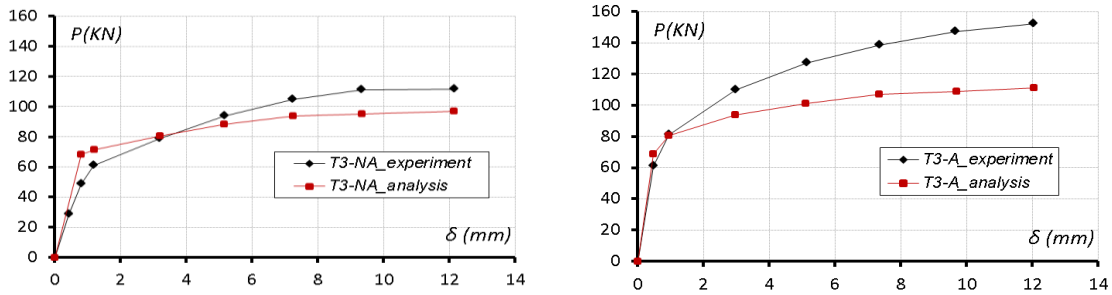

(a) T3 with no axial load (b) T3 with axial load

Fig. 20 Comparison of the P-δ skeleton curves obtained experimentally and analytically for the T3 frames

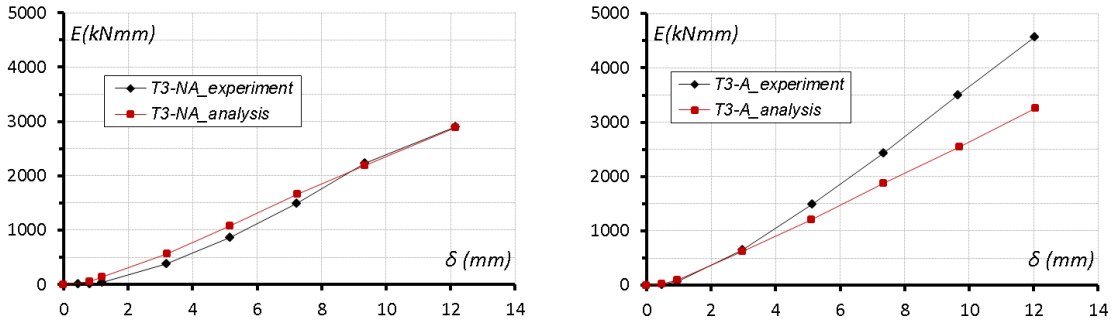

(a) T3 with no axial load (b) T3 with axial load

Fig. 21 Comparison of the numerical and experimental results for the dissipated energy of the T3 frames

results, whereas for the higher ones some discrepancies appear. However, it can be said that although the numerical *P-δ* curves, the *P-δ* skeleton curves and the dissipated energy present some differences with respect to the experimentally obtained ones, they can be considered acceptable, taking into account the nonlinear phenomena that are present in the physical model.

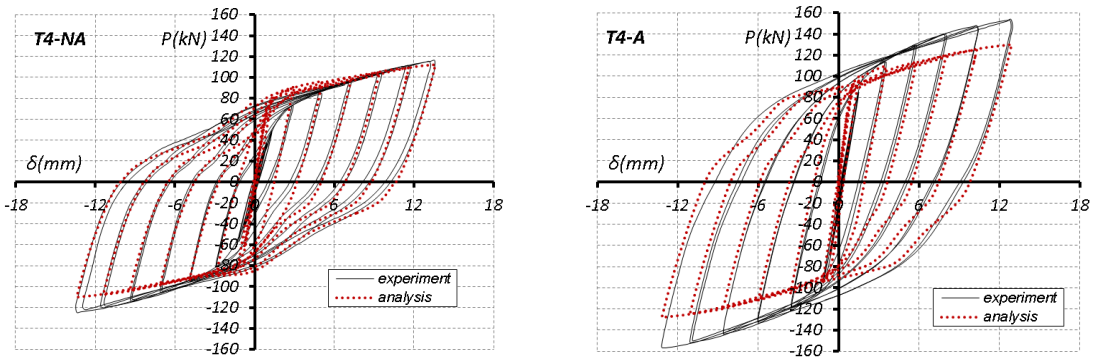

(a) T4 with no axial load (b) T4 with axial load

Fig. 22 Comparison of the numerical and experimental results for the T4 frames

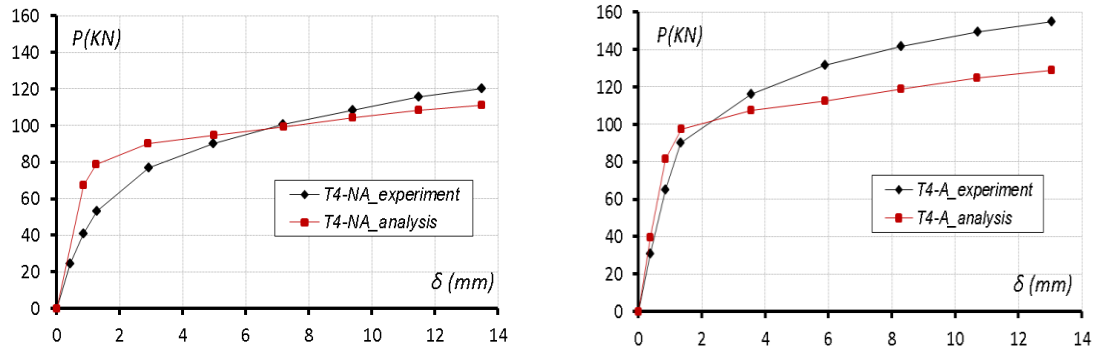

(a) T4 with no axial load (b) T4 with axial load

Fig. 23 Comparison of the *P-δ* skeleton curves obtained experimentally and analytically for the T3 frames

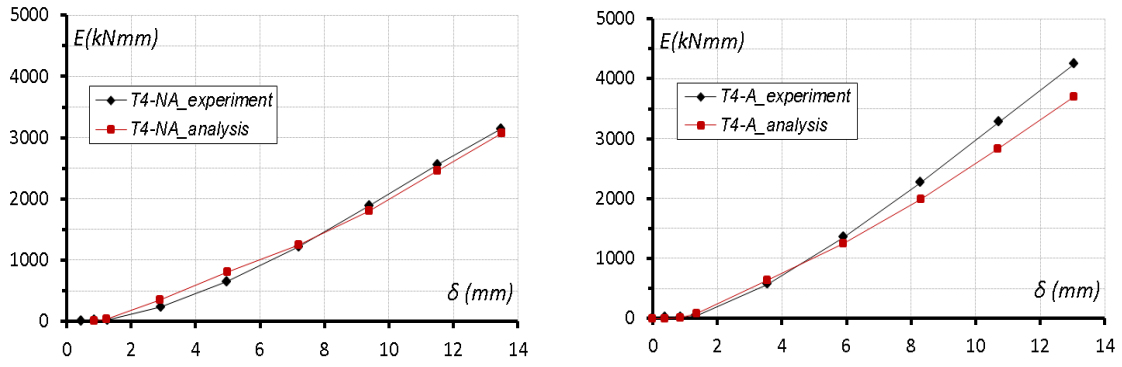

(a) T4 with no axial load (b) T4 with axial load

Fig. 24 Comparison of the numerical and experimental results for the dissipated energy of the T4 frames

4.4 Results for specimen T4

Similar conclusions can be drawn from the comparison of the numerical and experimental results presented in Figs. 22, 23 and 24, which concern the T4-NA strengthened frame (without axial load) and the corresponding T4-A strengthened frame (with axial load). Once again, the numerical and experimental results are in a rather good agreement, especially in terms of obtained load values and quality of the hysteresis loops.

4.5 General remarks on the results

In general, for the strengthened frames T2, T3 and T4, the numerical analyses produce results similar to the respective experimental ones, as far as the stiffness, the load values and the quality of the hysteresis loops are concerned. It can be concluded that the good agreement between the numerical and experimental results of these strengthened frames derives from the fact that in these cases the behaviour of the steel link element is dominant. In this case, the numerical model has the ability to simulate efficiently the isotropic and homogenous behaviour of the steel link element, as well as its stable elastoplastic deformation. On the other hand, the results obtained by analyses of the bare frame T1, present some differences compared to the experimental ones.

5. General comparison

From the comparison of the behaviour of the different frame specimens, interesting conclusions can be drawn. First of all, it is obvious from the experimental but also the numerical results that when the constant vertical load is applied on the columns of a frame, the obtained load values and the stiffness of this specimen are higher and the hysteresis loops are richer with respect to the corresponding specimen without the vertical axial load (see Figs. 13-24). Consequently, the dissipated energy is higher for the frames with the imposed axial force. In fact, it can be observed that the increase of the load bearing capacity of all the frames with the axial load lies in the range of 20-40 kN. These more or less standard differences can be attributed to the standard increase of the load bearing capacity of the columns after the imposition of the axial load. This holds for all the frames studied here, both the bare and the strengthened ones, regardless of the type of the steel link that is utilized.

As far as the strengthened frames are concerned, due to the activation of the steel link, a significant increase of the strength, the stiffness and the energy dissipation capacity can be noticed, with respect to the bare frame. More specifically, the load bearing capacity of the strengthened specimens is three to four times higher than that of the T1 frame, depending on the type of the steel link utilized. Moreover, for all the strengthened frames, the hysteresis loops are very rich and no pinching occurs, leading to much higher values of dissipated energy with respect to the bare frame.

Finally, after comparing the results obtained for the strengthened frames, it appears that the specimens strengthened with the I-shaped cross-section links behave better than the frames strengthened with the rectangular cross-section link. As it was clearly observed, especially during the experiments, the presence of the flanges in the I-shaped cross-section links prevented any distortion phenomena that were developed to the rectangular cross-section link. The contribution of the flanges resulted in higher strength, energy dissipation and mainly, deformation capacity for the respective strengthened frames.

6. Conclusions

In this study, two-dimensional numerical models are formulated for the simulation of tested RC frames strengthened with a specific bracing system which utilizes different types of dissipative link elements. The frames under study are subjected to horizontal cyclic loading with and without additional axial force on the columns.

After the comparison of the results obtained by the analyses and the respective tests, it can be concluded that, in general, there is a rather good approximation between the numerical and the experimental curves, especially for the strengthened frames, as in these cases the behaviour of the steel link is dominant and can be accurately reproduced by the proposed numerical models. Moreover, the numerical model is able to reproduce the plastic strain fields that develop in the steel links. For every case treated here, the picture of the plastic strain fields obtained by the analyses is compatible with the deformation of the link observed during the respective tests, as well as with the type of failure that each link exhibited at the end of the experiments.

Finally, both the experimental and the numerical results show that the use of the steel link elements can increase considerably the strength, the stiffness, but mainly the energy dissipation capacity of the frame. The beneficial effect of the imposed axial loads on the columns, on the behaviour of each studied frame, becomes evident also from the numerical and experimental results.

Acknowledgments

The work presented here is part of a broader program, partially sponsored by the Greek Earthquake Planning and Protection Organization (EPPO), the contribution of which is gratefully acknowledged.

References

Abdollahi, A. (1996), "Numerical strategies in the application of FEM to RC structures", *Comput. Struct.*, **58**(6), 1171-1182.

Antonucci, A., Balducci, F., Bartera, F., Castellano, G. and Chaudat, T. (2006), "Shaking table tests on RC frame braced with fluid viscous dampers", *Proceedings of the 1st European Conference of Earthquake Engineering and Seismology*, Geneva, Switzerland, September.

D' Aniello, M. (2006), "Seismic upgrading of RC structure by steel eccentric bracing (an experimental and numerical study)", *Pollack Periodica*, **1**(2), 17-32.

De Borst, R. and Nauta, P. (1985), "Non-orthogonal cracks in a smeared finite element model", *Eng. Comput.*, **2**(1), 35-46.

Georgiadi-Stefanidi, K., Mistakidis, E., Perdikaris, P. and Papatheocharis, T. (2010), "Numerical simulation of tested reinforced concrete beams strengthened by thin fibre-reinforced cementitious matrix jackets", *Earthq. Struct.*, **1**(4), 354-370.

Georgiadi-Stefanidi, K., Mistakidis, E., Perdikaris, P. and Papatheocharis, T. (2011), "Numerical simulation of the nonlinear bending response of fibre-reinforced cementitious matrix beams and comparison with experimental results", *Eng. Struct.*, **33**(12), 3579-3589.

Karalis, A.A., Georgiadi-Stefanidi, K.A., Salonikios, T.N., Stylianidis, K.C. and Mistakidis, E.S. (2011), "Experimental and numerical study on the behaviour of high dissipation metallic devices for the

strengthening of existing structures", *III ECCOMAS Thematic Conference on Computational Methods in Structural Dynamics and Earthquake Engineering*, *COMPDYN*, Corfu, Greece.

Karalis, A.A., Stylianidis, K.C. and Salonikios, T.N. (2010), "Experimental investigation of old R/C frames strengthened against earthquakes by high dissipation steel link elements", *Urban Habitat Constructions Under Catastrophic Events*, *Cost Action C26 FINAL Conference*, Balkema.

Karalis, A.A. and Stylianidis, K.C. (2013), "Experimental investigation of existing R/C frames strengthened by high dissipation steel link elements", *Earthq. Struct.*, **5**(2),143-160.

Kontoleon, M.J., Mistakidis, E.S., Baniotopoulos, C.C. and Panagiotopoulos, P.D. (1999), "Parametric analysis of the structural response of steel base plate connections", *Comput. Struct.*, **71**(1), 78-103.

Kunishue, A., Koshika, S., Kurokawa, Y., Suzuki, N., Agami, J. and Sakamoto, M. (1983), "Retrofitting method of existing reinforced concrete buildings using elasto-plastic steel dampers", *Proceeding of the12th World Conference on Earthquake Engineering*, New Zealand.

Mistakidis, E.S., Baniotopoulos, C.C., Bisbos, C.D. and Panagiotopoulos, P.D. (1997), "Steel T-stub connections under static loading: an effective 2D numerical model", *J. Constr. Steel Res.*, **44**(1-2), 51-67.

MSC Software Corporation (2010), *MSC Marc, Volume A: Theory and User Information.*

Perera, R., Gomez, S. and Alarcon, E. (2004), "Experimental and analytical study of masonry infill reinforced concrete frames retrofitted with steel braces", *J. Struct. Eng.- ASCE*, **130**(12), 2032-2039.

Pinto, A. and Taucer, F. (2006), *Assessment and retrofit of full scale models of existing RC frames*, Advances in Earthquake Engineering for Urban Risk Reduction, Springer.

Rabczul, T., Akkerman, J. and Eibl, J. (2005), "A numerical model for reinforced concrete structures", *Int. J. Solids Struct.*, **42**(5-6), 1327-1354.

Sickert, J.U., Kaliske, M., Graf, W. and Mandara, A. (2010), "Robust design of seismic upgrading of RC structure with innovative bracing systems", *Urban Habitat Constructions Under Catastrophic Events*,*COST Action C26 FINAL CONFERENCE*, Balkema.

Wang, C.Y., Ho, H.Y., Wang, R.Z. and Huang, H.H. (2008), "Numerical simulations of non-ductile RC frames with infilled brick panel under cyclic loading", *J. Chin. Inst. Eng.*, **31**(5), 827-840.